Effects of Complex Formation on Vibrational Circular Dichroism Spectra

Valentin Paul Nicu,*,† Johannes Neugebauer,‡ and Evert Jan Baerends*,†

Theoretical Chemistry, Vrije Universiteit Amsterdam, De Boelelaan 1083, 1081 HV Amsterdam, The Netherlands, and Laboratorium für Physikalische Chemie, ETH Zurich, Wolfgang-Pauli-Strasse 10, 8093 Zurich, Switzerland

Received: October 21, 2007; Revised Manuscript Received: March 3, 2008

The determination of absolute configurations of chiral compounds using VCD is performed by comparing measured vibrational circular dichroism (VCD) spectra with calculated spectra. The process is based on two facts: the two enantiomers have rotational strengths of opposite sign, and the absolute configuration of the molecule used in the calculation is known. However, calculations on isolated molecules very often predict VCD intensities of very different magnitude or even different signs compared to the spectra measured in solution. Therefore, we have carefully analyzed what type of changes are induced by complexation of a solvent molecule to a solute. In the theoretical example of benzoyl-benzoic acid (in a particular chiral conformation) hydrogen bonded to the achiral NH_3, we distinguish six cases, ranging from no or very small changes in the rotational strengths of solute modes (case **A**) to changes of sign of rotational strengths (case **B**), changes in magnitude (case **C**), nonzero rotational strengths for modes of the achiral solvent ("transfer of chirality", case **D**), large frequency shifts accompanied by giant enhancements of the IR and VCD intensities of modes involved in hydrogen bonding (case **E**), and emergence of new peaks (case **F**). In this work, all of these situations will be discussed and their origin will be elucidated. On the basis of our analysis, we advocate that codes for VCD rotational strength calculation should output for each mode i the angle $\xi(i)$ between the electric and magnetic transition dipole moments because only "robust modes" with ξ far from 90° should be used for the determination of the absolute configuration.

Introduction

The significant advances made in the past decades in both experimental techniques[1] and quantum mechanical ab initio calculations[2] of vibrational circular dichroism (VCD) intensities has made VCD a very successful spectroscopic technique for the determination of the absolute configuration (AC) of chiral molecules. Knowledge of the AC is of utmost importance in the pharmaceutical industry because the enantiomers of chiral drugs can have significantly different biological and pharmacological properties.

In the case of VCD spectroscopy, the discrimination between the enantiomers is based on the fact that they have VCD intensities of equal magnitude but opposite sign. The AC is established by comparing the experimental spectrum, usually measured in solution, to a calculated spectrum obtained from a DFT calculation. The AC of the enantiomer used in the calculation is known. Thus, if the main features of the experimental and calculated VCD spectra have the same sign, then the experimental sample has the same AC as the enantiomer used in the simulation; if the signs are different, then so is the AC.

Because the DFT calculations are usually done for isolated molecules, knowledge and understanding of the mechanisms that may affect the VCD intensities in solution, and therefore possibly hinder the determination of the AC from gas-phase calculations, are of great importance. In the last few years, the number of studies investigating the effect of hydrogen-bonded complex formation on the VCD spectra has increased rapidly.[3–17] Given the importance of hydrogen-bonding intermolecular interactions, such as solute−solvent and solvent−solvent, these studies have addressed questions such as elucidation of structural information of the molecular complex from VCD spectra, and the appearance of water modes in the VCD spectrum ("transfer of chirality"). These studies have also demonstrated that long-range dielectric effects, as given by a polarizable continuum model for the solvent, are not sufficient to model the solvation effect on the spectra; explicit hydrogen-bonding has to be taken into account.

Because the formation of a molecular complex between a solute molecule and a solvent molecule will be the most important interaction causing perturbation of the VCD signals compared to the gas phase, in this paper we will investigate in detail the effects of complexation on the VCD signals. We will consider the example of a molecular complex formed from the chiral 2-benzoyl benzoic acid (BBA) (the "solute") and the achiral NH_3 (the "solvent" molecule). The NH_3 is hydrogen bonded to the hydrogen of the carboxylic acid group of BBA. Our interest is not primarily in this specific system, but we study it as a convenient model for the effects of molecular complex formation. The BBA-(−)-(*R*) -amphetamine complex has been studied in connection with the induced (electronic) CD effect,[18,19] and our present investigation has started by replacing the amphetamine, whose amino group acts as hydrogen acceptor in the hydrogen bond with the carboxylic OH group of BBA, by the simple nonchiral NH_3 molecule, which forms a similar hydrogen bond with BBA. We now take this NH_3 molecule as a prototype hydrogen-bonding solvent molecule, and we will study the effect of this particular intermolecular interaction on the VCD spectrum in detail. It should be noted that this system is an entirely theoretical model because BBA is not chiral in a

* Corresponding authors. E-mail: nicu@chem.vu.nl; baerends@chem.vu.nl.
† Vrije Universiteit Amsterdam.
‡ ETH Zurich.

10.1021/jp710201q CCC: $40.75
Published on Web 07/08/2008

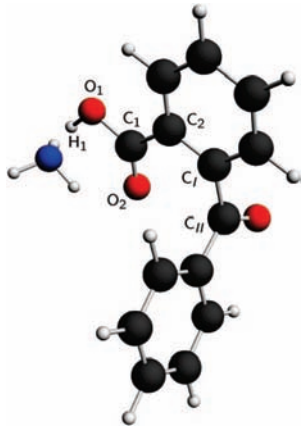

Figure 1. Optimized (BP86/TZP) geometry of the BBA−NH_3 complex.

dynamical sense. In solution, both enantiomers will exist with equal probability because they can be obtained from each other by a low-barrier rotation of 180° around the C_I-C_{II} bond (see Figure 1). However, the optimized conformer of BBA used as a model system in this work is of course chiral and therefore well suited to study the changes induced in the VCD spectra by complex formation. The conclusions of this study may therefore be generalized to other solvent−solute molecular complexes involving chiral donors and/or acceptors. We will, indeed, occasionally illustrate our findings with the water-lactic acid and methyl−lactate−water complexes studied before.[12,14] We should mention that besides the BBA−NH_3, methyl lactate−H_2O, and D-lactic acid−H_2O molecular complexes, we have analyzed other chiral molecular complexes, such as benzaldehyde−H_2O, benzaldehyde−NH_3, benzoic acid−H_2O, benzoic acid−NH_3, BBA−H_2O, amphetamine−H_2O, and amphetamine−BBA. We considered BBA−NH_3 as the prototype molecular complex for our paper because among the studied complexes it was the only one that exhibited all of the mechanisms we have found to be responsible for changing the VCD intensities.

The various effects that are observed—for example, changes in magnitude of the rotational strength, or changes in the sign of the rotational strength of some modes, large shifts in frequency that are accompanied by a huge enhancement of the IR/VCD intensities of some modes—will be classified, and their origin will be elucidated. A thorough understanding of these phenomena is not only of intrinsic interest but also of practical interest because it can provide insight into the modes for which the discrepancies between experiment and theory can be ascribed to complex formation effects with solvent molecules.

When forming a molecular complex, an induced VCD effect defined as the difference between the VCD of the combined system and the two individual systems, is always to be expected because the molecular complex has six additional normal modes compared to the free monomers, $6 = 3(N_1 + N_2) - 6 - (3N_1 - 6) - (3N_2 - 6)$ (N_1 and N_2 are the number of atoms of the two monomers). However, most of these additional modes are intermolecular modes at low frequencies where VCD measurements are not feasible. It is therefore expected that these modes will not hinder the process of determining the AC. More significant changes of the VCD spectra, which can make the comparison of experimental and calculated spectra difficult, are expected because of perturbations in the geometries and electronic structures of the two monomers. These perturbations will be reflected in changes of the normal modes and in changes in the electronic contributions of the atomic polar and the atomic axial tensors. Ultimately, these perturbations translate into changes of the magnitude and orientation of the total electric and magnetic transition dipole moments, which will result in modifications of the VCD intensities.

This article is organized as follows: in the next two sections we will present the theory of VCD and the approach we use for describing the effect of complexation on the VCD spectra. Then we analyze in detail the types of changes in a VCD spectrum that can result from complex formation and the mechanisms that can induce such changes. Finally, the results are summarized along with some concluding remarks.

Theory

The VCD intensity for the fundamental transition ($|0\rangle \rightarrow |1\rangle$) of the ith vibrational mode is given by the rotational strength (R):[20]

$$R(i) = \vec{E}_{01}(i) \cdot Im[\vec{M}_{10}(i)] \tag{1}$$

where $\vec{E}_{01}(i)$ and $\vec{M}_{10}(i)$ are the electric and magnetic transition dipole moments of the first vibrational transition of the ith normal mode. The sign of the rotational strength is determined by the angle $\xi(i)$ between the vectors $\vec{E}_{01}(i)$ and $\mathrm{Im}[\vec{M}_{10}(i)]$ (which is a real vector because $\vec{M}_{10}(i)$ is purely imaginary):

$$\cos\xi(i) = \frac{\vec{E}_{01}(i) \cdot Im[\vec{M}_{10}(i)]}{|\vec{E}_{01}(i)||Im[\vec{M}_{10}(i)]|} \tag{2}$$

where $|\vec{E}_{01}(i)|$ and $|\mathrm{Im}[\vec{M}_{10}(i)]|$ are the lengths of the vectors $\vec{E}_{01}(i)$ and $\mathrm{Im}[\vec{M}_{10}(i)]$, respectively. Thus, if $\xi < 90°$, then $R(i) > 0$; if $\xi > 90°$, then $R(i) < 0$.

The transition dipole moments $\vec{E}_{01}(i)$ and $\vec{M}_{10}(i)$ can be written as a sum of contributions from each atom:

$$\vec{E}_{01}(i) = \sum_{\lambda} \vec{E}^{\lambda}_{01}(i), \qquad \vec{M}_{10}(i) = \sum_{\lambda} \vec{M}^{\lambda}_{10}(i) \tag{3}$$

Within the harmonic approximation, the atomic contributions of the electric and magnetic transition dipole moments are given by:[20,21]

$$(\vec{E}^{\lambda}_{01})_{\beta}(i) = \left(\frac{\hbar}{\omega_i}\right)^{1/2} \sum_{\alpha} \vec{S}^{\lambda}_{\alpha}(i) P^{\lambda}_{\alpha\beta} \tag{4}$$

$$(\vec{M}^{\lambda}_{10})_{\beta}(i) = -(2\hbar^3\omega_i)^{1/2} \sum_{\alpha} \vec{S}^{\lambda}_{\alpha}(i) \vec{M}^{\lambda}_{\alpha\beta} \tag{5}$$

In eqs 4 and 5, $\hbar$ is the reduced Planck constant, ω_i is the frequency of the ith vibrational mode, $P^{\lambda}_{\alpha\beta}$ and $M^{\lambda}_{\alpha\beta}$ are the atomic polar tensor (APT) and the atomic axial tensor (AAT), $S^{\lambda}_{\alpha}(i)$ is the transformation matrix from Cartesian to normal coordinates (the nuclear displacement vectors of the ith normal mode), α and β denote Cartesian coordinates, and λ labels the nuclei. As can be seen from eqs 4 and 5, the transition dipole moments are determined by the atomic tensors $P^{\lambda}_{\alpha\beta}$ and $M^{\lambda}_{\alpha\beta}$ and by the nuclear displacement vectors, $S^{\lambda}_{\alpha}(i)$. Thus, the contribution to the total dipole transition moments E_{01} and M_{01} from an atom that is not moving in a given normal mode is zero because the nuclear displacement vectors of such an atom are zero.

Both tensors, APT and AAT, are defined per atom and have electronic and nuclear contributions:[21]

$$P^{\lambda}_{\alpha\beta} = E^{\lambda}_{\alpha\beta} + N^{\lambda}_{\alpha\beta} \quad (6)$$

$$M^{\lambda}_{\alpha\beta} = I^{\lambda}_{\alpha\beta} + J^{\lambda}_{\alpha\beta} \quad (7)$$

The electronic contributions are

$$E^{\lambda}_{\alpha\beta} = \left(\frac{\partial \langle \psi_G(R) | (\hat{\mu}_E)_\beta | \psi_G(R) \rangle}{\partial R_{\lambda\alpha}} \right)_{R^0} \quad (8)$$

$$I^{\lambda}_{\alpha\beta} = \left\langle \left(\frac{\partial \psi_G(\mathbf{R})}{\partial R_{\lambda\alpha}} \right)_{\mathbf{R}^0} \middle| \left(\frac{\partial \psi_G(\mathbf{R}^0, \mathbf{H})}{\partial H_\beta} \right)_{\mathbf{H}=0} \right\rangle \quad (9)$$

The nuclear contributions are

$$N^{\lambda}_{\alpha\beta} = eZ_\lambda \delta_{\alpha\beta} \quad (10)$$

$$J^{\lambda}_{\alpha\beta} = i \frac{eZ_\lambda}{4\hbar c} \sum_\gamma \varepsilon_{\alpha\beta\gamma} R^0_{\lambda\gamma} \quad (11)$$

In eqs 8−11, eZ_λ and R_λ are the charge and the position of nucleus λ, R^0_λ is R_λ at the equilibrium geometry, H is a static magnetic field, $\varepsilon_{\alpha\beta\gamma}$ is the Levi−Civita tensor, the indices α, β, and γ run over Cartesian components, e and c are the elementary charge and the speed of light in vacuum, and ψ_G is the electronic wave function of the ground state G. In eq 9, $\Psi_G(R)$ depends on the positions of the nuclei, which are not fixed, whereas $\Psi_G(R^0, H)$ has to be calculated for the equilibrium positions of the nuclei in the presence of a magnetic field.

Method

From eqs 1−5, the rotational strengths are determined by the atomic tensors $P^{\lambda}_{\alpha\beta}$ and $M^{\lambda}_{\alpha\beta}$ and by the nuclear displacement vectors $S^{\lambda}_{\alpha}(i)$. Thus, to identify and understand the mechanisms behind the changes induced in the VCD spectra by complexation, we monitor the changes of the AATs, APTs, normal modes, and of the resulting electric and magnetic transition dipole moments when going from the free molecule to the molecular complex. Unless otherwise specified, NH_3 is considered a perturbation and only the atomic tensors, the nuclear displacement vectors, and the transition dipole moments of the BBA atoms are investigated. The AATs and the magnetic transition dipole moments are origin-dependent. Thus, in order to compare these two quantities in the free monomers (FM) and in the molecular complex (MC), we took care to preserve the position of the center of mass of the two monomers and their orientation in the coordinate systems of the FM and of the MC.

The changes induced in the atomic tensors (APTs, AATs) are investigated by means of correlation diagrams. In such a diagram, (x, y) points are plotted for all tensor components of all of the atoms of BBA, with the x value being the tensor component in the free BBA and the y value being the corresponding tensor component of the BBA in the BBA−NH_3 complex. Perfect equality will yield a straight line with a slope of 1.

The extent to which a normal mode was affected by complexation is estimated by calculating an overlap of the nuclear displacement vectors of the atoms of BBA in the free molecule and in the molecular complex. For each normal mode a $3N$-dimensional vector, with N being the number of atoms of the molecule ($N = 27$ for BBA, $N = 31$ for BBA−NH_3), is constructed using the Cartesian components of the displacement vectors of all atoms:

$$\vec{V}(i) = \vec{V}(v^1_x(i),\ v^1_y(i),\ v^1_z(i), \ldots,\ v^N_x(i),\ v^N_y(i),\ v^N_z(i)) \quad (12)$$

where $V(i)$ is the $3N$-dimensional vector associated with the mode i, and $v^{\lambda}_k(i)$ is the kth Cartesian component of the displacement vector of atom λ in the normal mode i. The vector $\vec{V}(i)$ is then normalized

$$\vec{V}(i) = \frac{\vec{V}(i)}{|\vec{V}(i)|} \quad (13)$$

where $|\vec{V}(i)|$ is the length of the vector $\vec{V}(i)$. For a pair of normal modes i and j, such a normalized vector is calculated for both the free molecule, $\vec{V}(i)$, and the molecular complex, $\vec{U}(j)$. The overlap of the modes i and j, $\Omega(i, j)$, is obtained by calculating the scalar product of vectors $\vec{V}(i)$ and $\vec{U}(j)$:

$$\Omega(i,\ j) = \vec{V}(i) \cdot \vec{U}(j) = \frac{\sum_{\lambda=1}^{N} \sum_k^{x,\ y,\ z} v^{\lambda}_k(i)\ u^{\lambda}_k(j)}{|\vec{V}(i)||\vec{U}(j)|} \quad (14)$$

Note that in eq 14 the summation index λ runs only over the BBA atoms ($N = 27$). The value of the scalar products $\Omega(i, j)$ gives an indication of how well the nuclear displacement vectors of the modes i and j overlap. Two identical modes yield an overlap of 1. Thus, the closer Ω is to 1, the more the displacement vectors in the free molecule and in the molecular complex resemble each other.

When comparing a mode of free BBA to the corresponding one in the complex, the differences between the total electric and magnetic transition dipole moments of the modes are also analyzed by comparing their Cartesian components. To understand the origin of the differences, we closely investigate the differences in the normal coordinates, that is, which atoms move differently in the two normal modes, the type of the normal modes, and the correlation diagrams for the atomic tensors.

Finally, the rotational strength in the complex is broken down into intra- and interfragment contributions by writing the total electric and magnetic transition dipole moments of the molecular complex as a sum of contributions from the two monomers:

$$\begin{aligned} R(i) &= \mathrm{Im}\{[\vec{E}^A_{01}(i) + \vec{E}^B_{01}(i)] \cdot [\vec{M}^A_{10}(i) + \vec{M}^B_{10}(i)]\} \\ &= \mathrm{Im}[\vec{E}^A_{01} \cdot \vec{M}^A_{10} + \vec{E}^A_{01} \cdot \vec{M}^B_{10} + \vec{E}^B_{01} \cdot \vec{M}^A_{10} + \vec{E}^B_{01} \cdot \vec{M}^B_{10}] \\ &= R^{AA}(i) + R^{AB}(i) + R^{BA}(i) + R^{BB}(i) \end{aligned} \quad (15)$$

In eq 15, the upper indices A and B label the two monomers; $\vec{E}^A_{01}(i)$ and $\vec{M}^A_{10}(i)$ are the electric and magnetic transition dipole moments of fragment A associated to the first vibrational transition of mode i, obtained by summing in eq 3 over the atoms λ of A. The term $R^{XY}(i) = \mathrm{Im}[\vec{E}^X_{01} \cdot \vec{M}^Y_{10}\ ]$ is the contribution to $R(i)$ due to $\vec{E}^X_{01}(i)$ and $\vec{M}^Y_{10}(i)$, where $X, Y = \{A, B\}$. The terms $R^{AA}(i)$ and $R^{BB}(i)$ are the contributions to $R(i)$ due to the monomers A and B, respectively, whereas the cross terms $R^{AB}(i)$ and $R^{BA}(i)$ are the contributions due to couplings between the electric and magnetic transition dipole moments of the two monomers.

In the next section, the results of the detailed analysis outlined here are presented. As will be shown, this type of analysis enables an understanding of the changes induced by complexation in the VCD spectra.

All of the calculations (geometry optimization and IR/VCD calculations) are performed using the ADF program package.[22–24] The vibrational rotational strengths are calculated using our recent implementation[25] of Stephens' equations for VCD[20] in the ADF program. The geometries are optimized using the QUILD program[26] of ADF. Analytical derivative techniques[27–29] are employed for the calculation of the APTs, AATs and harmonic force field, within the framework of density functional theory. For the calculation of AATs, London atomic orbitals

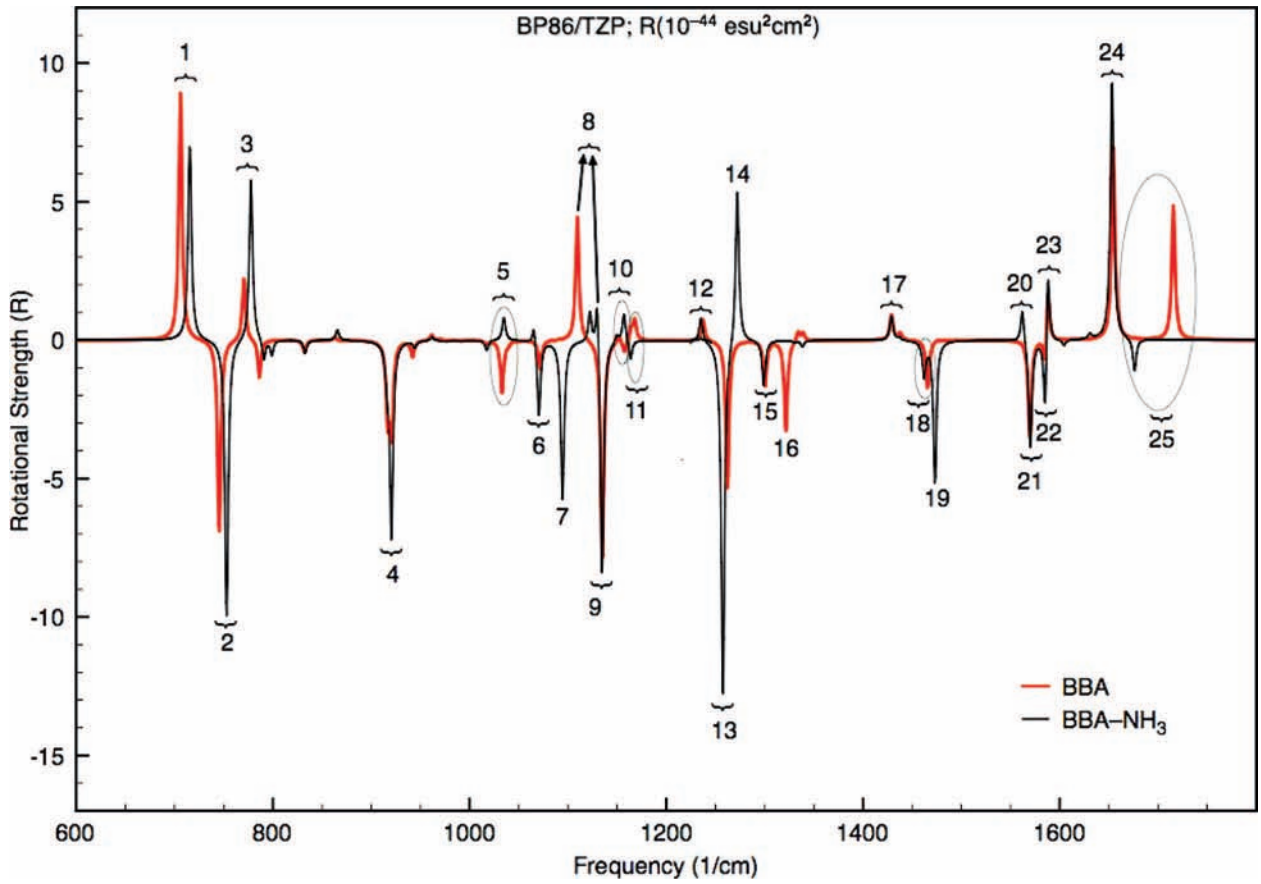

Figure 2. VCD spectra (BP86/TZP) of BBA and BBA−NH_3 for the frequency interval between 600 and 1800 cm^{-1}.

based on Slater-type orbitals and the common origin gauge are used. The BP86 functional and the TZP basis set are used in all of the calculations. The analysis outlined in this section was carried out using the ToolsVCD program, a FORTRAN code written by the authors. ToolsVCD requires data saved during an ADF IR/VCD calculation.

Complex Formation Effects on the VCD Spectrum of the BBA−NH_3 Molecular Complex

When comparing the calculated and experimental spectra of a given molecule, a one-to-one mapping between the VCD signals of the two spectra must be established first. Assuming this has been done, and all pairs of corresponding normal modes would have VCD intensities of the same sign and about the same magnitude, the identification would pose no problem. However, one can often distinguish pairs that have VCD intensities of the same sign but of different magnitudes and pairs that have VCD intensities of different signs. Besides differences in intensities, other differences may also occur between the compared spectra: shifts in the frequencies of the normal modes, the presence of additional lines in the experimental spectrum (e.g., modes of the solvent), and huge enhancements of the intensities of some of the modes. In this work, all of these situations will be encountered as a result of solute−solvent complex formation. We will use the calculated VCD spectra of the free BBA and the BBA−NH_3 molecular complex to analyze why such different effects of complex formation are observed for different modes and how they arise.

The BBA−NH_3 molecular complex is depicted in Figure 1. The calculated VCD spectra of BBA and BBA−NH_3 are shown in Figure 2 for the frequency range between 600 and 1800 cm^{-1}, and in Figure 3 for the range between 600 and 3600 cm^{-1}. As can be seen, the VCD spectrum of BBA is significantly affected by the complexation with NH_3. The pairs of corresponding normal modes in the two spectra are labeled with numbers from 1 to 26. Only the pairs with significant VCD intensities have been labeled. The frequencies, rotational strengths, and normal-mode overlaps (Ω) for all of the pairs of normal modes labeled are given in Table 1. Each pair of normal modes has been analyzed according to the procedure outlined in the previous section. The results clearly show that when analyzing differences/similarities between/of two VCD spectra one can distinguish between six distinct situations. We have labeled these six cases with letters from *A* to *F*. For each case, 1 or 2 representative examples out of the 26 modes in Table 1 are discussed here. For the rest of the modes, tables containing all of the quantities relevant for their analysis are given in the Supporting Information (SI). The unit of the rotational strengths is 10^{-44} $esu^2 \cdot cm^2$. For brevity, in what follows only the values (without units) of the rotational strengths will be given.

First the atomic tensors are investigated. In Figures 4 and 5, the correlation diagrams for the APTs and the AATs of BBA, respectively, are shown. As can be seen, the correlations for both AATs and APTs are very good, which indicates that the atomic tensors are affected very little by complexation. We have verified that the few tensor components that show small deviations from the 45° line (see Figures 4 and 5) belong to the atoms that are in the vicinity of the intermolecular bonding area (the atoms H_1, O_1, O_2, C_1, C_2 in Figure 1).

An analysis of the normal modes of BBA−NH_3, BBA, and NH_3 showed that the modes of BBA−NH_3 can be classified as modes that are specific to BBA (are also found in the free BBA)

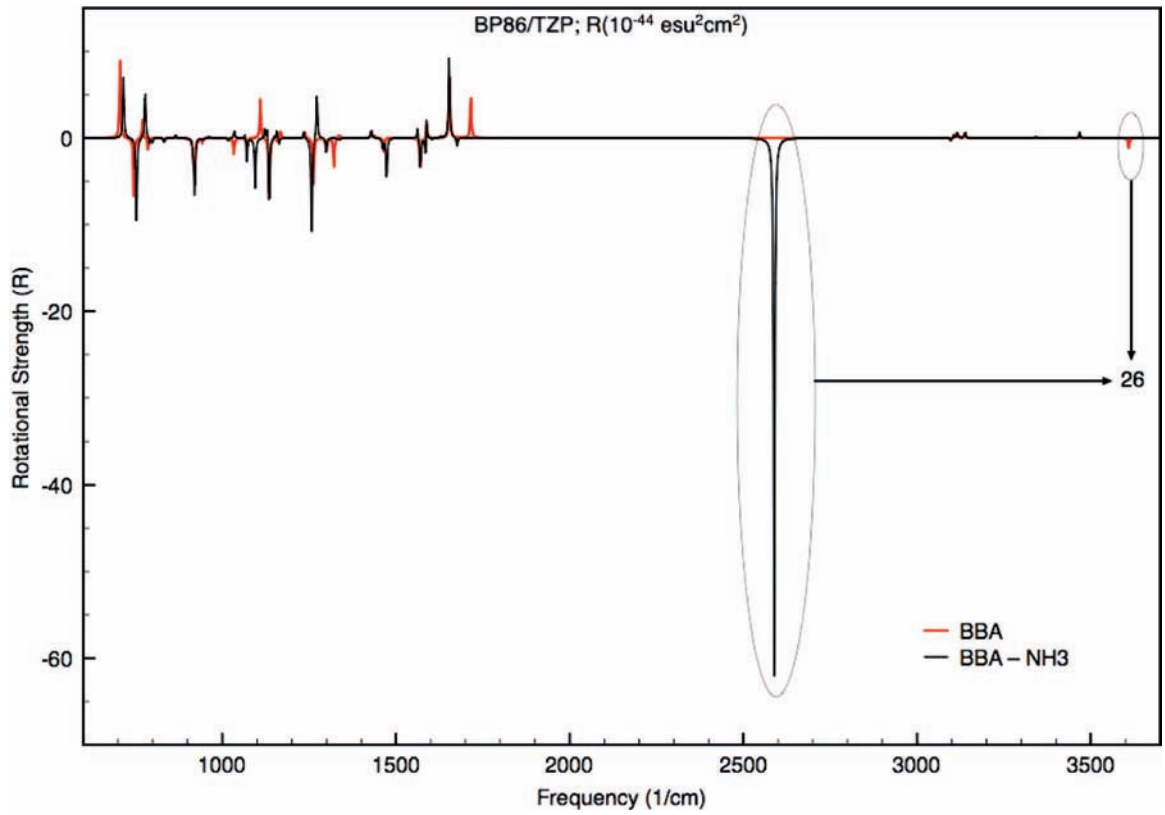

Figure 3. VCD spectra (BP86/TZP) of BBA and BBA−NH_3 for the frequency interval between 600 and 3700 cm^{-1}.

TABLE 1: Frequencies (cm^{-1}) and Rotational Strengths (10^{-44} $esu^2 \cdot cm^2$) for the Modes of BBA and BBA−NH_3 Labeled in Figures 2 and 3[a]

	BBA−NH_3		BBA/*NH_3			
no.	freq	*R*	freq	*R*	Ω	case
1	715.5	44.7	706.3	58.0	0.88	**C**
2	752.9	−63.1	745.4	−44.2	0.97	**C**
3	777.7	36.9	770.7	13.4	0.74	**C**
4	920.6	−44.0	920.5	−19.9	0.91	**C**
5	1034.9	5.2	1033.1	−10.8	0.84	**B**
6	1070.5	−17.4	1071.7	−6.5	0.97	**C**
7	1094.5	−36.7	*1033.1	0.0	0.99	**D**
8	1129.9	14.4	1109.7	28.2	0.59	**C**
9	1134.6	−55.6	1135.1	−49.6	0.86	**C**
10	1156.9	6.5	1157.7	−2.6	0.96	**B**
11	1163.5	−4.5	1168.2	4.9	0.41	**B**
12	1235.2	5.5	1237.5	5.5	0.99	**A**
13	1257.6	−82.5	1262.4	−33.9	0.95	**C**
14	1272.1	35.0				**F**
15	1299.2	−10.3	1300.4	−10.7	0.99	**A**
16			1321.9	−19.8		**F**
17	1428.9	5.5	1429.0	5.6	0.99	**A**
18	1462.1	−7.9	1465.6	−11.2	0.74	**C**
19	1473.3	−34.5				**F**
20	1561.9	7.9	1560.7	0.0	0.99	**C**
21	1570.1	−25.1	1569.7	−22.3	0.99	**A**
22	1585.4	−22.5	1585.2	−7.7	0.99	**C**
23	1587.7	22.5	1588.1	12.5	0.99	**C**
24	1653.2	59.5	1654.6	42.6	0.99	**C**
25	1676.0	−7.3	1716.1	33.1	0.90	**B**
26	2588.9	−402.4	3608.4	−7.9	0.99	**E**

[a] The overlap of the normal modes (Ω) and the case to which each pair of modes belongs is also given. Note that * denotes a NH_3 mode.

(cases **A**, **B**, **C**, and **E** below), modes that are specific to NH_3 (are found also in the free NH_3) (case **D** below), and modes

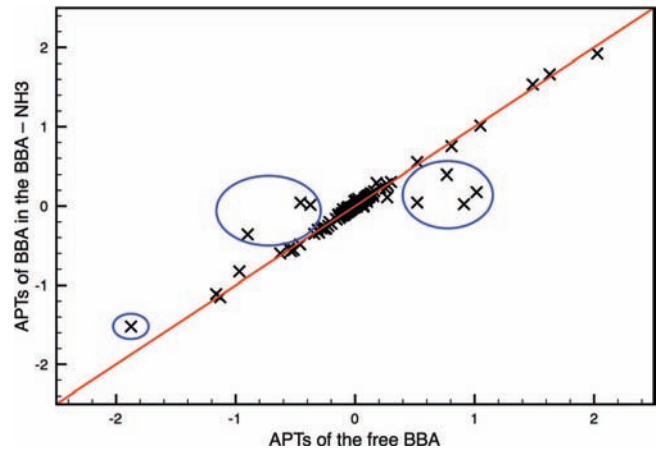

Figure 4. Correlation diagrams for the tensor components of the APTs of the BBA atoms. Encircled entries represent APT components of the atoms H_1, O_1, O_2, C_1, C_2 in Figure 1.

that are specific to the MC and have no counterpart in the free monomers (case **F** below).

Case **A** represents the modes of BBA that are affected very little by complexation. A common feature of all of the modes of type *A* is that the atoms of BBA near the intermolecular bonding area and the atoms of NH_3 are not involved in the normal mode motion; they are practically frozen in these modes. The modes of type *A* involve very similar motions of BBA atoms in the free BBA and in the complex; they exhibit values of the overlap Ω that are very close to 1. Because only the atoms with virtually unchanged APTs and AATs are engaged in the normal mode motion, very small differences result between the VCD intensities of the mode in BBA−NH_3 and in BBA.

As an example, the pair of normal modes number 15 (see Table 1) is considered. The modes in this pair are characterized

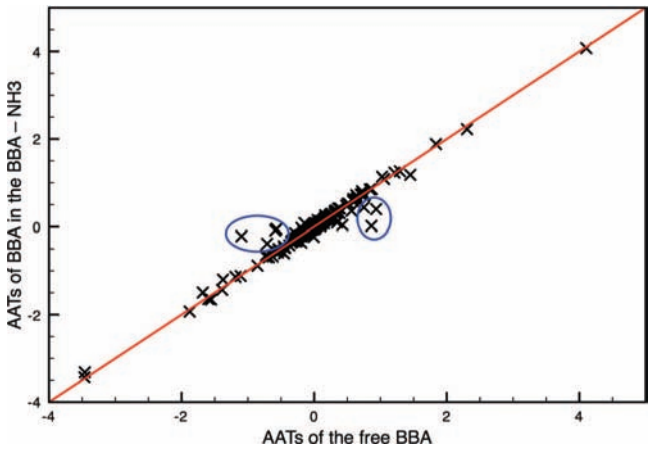

Figure 5. Correlation diagram for the tensor components of the AATs of the BBA atoms. Encircled entries represent AAT components of the atoms H_1, O_1, O_2, C_1, C_2 in Figure 1.

TABLE 2: Data Relevant for the Analysis of Pair 15 (Case A, Ω = 0.99) in Table 1[a]

(a) Frequency (cm^{-1}), R (10^{-44} $esu^2 \cdot cm^2$), ξ (deg)

	freq	R	ξ
free BBA:	1300.47	−10.71	94.00
BBA−NH_3:	1299.20	−10.37	94.26

(b) Im[$\vec{M}_{01}(i)$] (10^{-25} esu·cm)

	x	y	z
free BBA:	−208.27	180.37	12.73
BBA in MC:	−195.54	179.22	26.10
NH_3 in MC:	−0.08	0.10	−0.08

(c) $\vec{E}_{01}(i)$ (10^{-21} esu·cm)

	x	y	z
free BBA:	36.31	37.37	−19.58
BBA in MC:	34.36	34.41	−19.40
NH_3 in MC:	0.01	0.10	0.05

(d) Contributions R^{ij} (10^{-44} $esu^2 \cdot cm^2$) of R

		R^{ij}	ξ (deg)
BBA in MC:	R^{AA}	−10.58	94.35
coupling:	R^{AB}	0.02	73.43
coupling:	R^{BA}	0.18	52.32
NH_3 in MC:	R^{BB}	0.00	69.89

[a] Ω is the normal mode's overlap; (a) frequencies (freq), rotational strength (R), and the angle ξ; (b and c) Cartesian components of the magnetic, $\vec{M}_{01}(i)$, and electric, $\vec{E}_{01}(i)$, dipole transition moments of free BBA, of BBA in BBA−NH_3, and of NH_3 in BBA–NH_3, respectively; (d) the contributions R^{AA}, R^{AB}, R^{BA}, R^{BB} to R of BBA−NH_3, and their associated angle ξ.

by rocking movements of the hydrogen atoms of the benzoyl group in the plane of the benzene ring. All of the relevant data required for the analysis of this pair of modes are given in Table 2. The normal mode overlap is 0.99, meaning that the BBA mode is insignificantly affected by the complexation with NH_3. Next, the Cartesian components of the electric and magnetic transition dipole moments of BBA and BBA−NH_3 are compared. As can be seen from Table 2, they differ only very slightly. The reason for this is twofold. First, the normal modes did not change, and second, the atoms in the intermolecular bonding area (the ones with atomic tensors affected by complexation) are not moving in this normal mode and therefore their contributions to the transition dipole moments is zero. Finally, we look at the contributions of the rotational strength

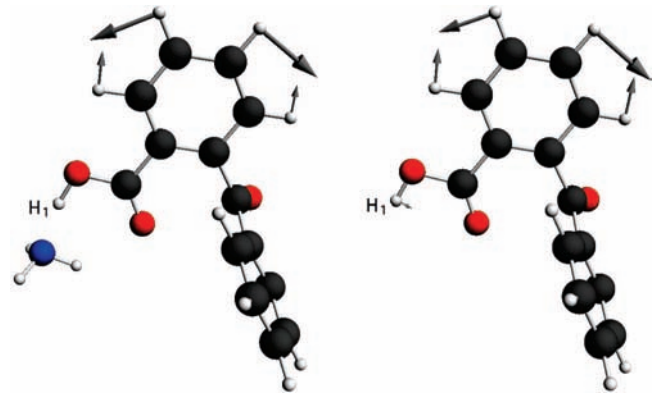

Figure 6. Nuclear displacement vectors for the normal modes of pair number 10 in Table 1.

(in Table 2). The only important contribution to rotational strength of the molecular complex comes from the term R^{AA}, the rest of the terms (R^{AB}, R^{BA}, R^{BB}) being negligible. The term R^{AA} represents the contribution from the BBA monomer. From Table 2, the term R^{AA} and its associated angle ξ have values that are very close to the values of their counterparts in the free BBA ($R^{AA} = -10.58$ and $\xi = 94.35°$ vs $R = -10.37$ and $\xi = 94.26°$). We therefore conclude that this particular mode of BBA is practically unaffected by the complexation with NH_3. As a result, it has approximately the same VCD intensity in the free molecule and in the molecular complex. This is characteristic for all of the modes of type *A*.

Case **B** describes modes that, although at almost the same frequency, have VCD intensities of different sign in BBA and in BBA−NH_3. This seems to be a significant discrepancy, but actually the absolute change is not very large. The BBA modes of this type are characterized by values of the angle ξ of eq 2 that are close to 90°. Thus, even a small perturbation may change the angle across the 90° value, which explains the sign change. The results of our analysis show that there are two different mechanisms responsible for changing the sign of the VCD intensity when going from the free molecule to the molecular complex. In the first mechanism, the displacements vectors and/or the atomic tensors of the BBA atoms may be sufficiently perturbed by the complexation that the electric and magnetic transition dipole vectors, although still arising (almost) exclusively from BBA atoms, change their magnitude and in particular their angle across 90°. In this case, only the intrafragment contribution R^{AA} (*A* is BBA) is significant, its value being different from the rotational strength of the free BBA. In the second mechanism, the BBA mode couples, even if weakly, to NH_3 modes, and the coupling terms R^{AB} and R^{BA}, which of course are totally absent in free BBA, have to be taken into account. They may even give rise to, or at least contribute significantly to, this effect of sign change. In the following, each mechanism is discussed by considering a specific example.

As an example of the first mechanism, we consider the normal mode pair number 10 in Table 1. The modes of pair 10 are characterized by rocking movements of the hydrogen atoms of the benzoic acid in the plane of the benzene ring. In BBA, the hydrogen atom labeled as H_1 in Figure 1 is also moving, but with smaller amplitude than the rest of the hydrogens. In BBA−NH_3 the hydrogen H_1, that is now involved in the intermolecular bond, is practically frozen, as are the atoms of NH_3. This can be seen clearly in Figure 6 where the two normal modes are depicted. The data relevant for the analysis of this pair of modes are given in Table 3. The overlap of normal modes is 0.96, indicating that except for the change for atom H_1 the

TABLE 3: Data Relevant for the Analysis of Pair 10 (Case B, Ω = 0.96) in Table 1[a]

(a) Frequency (cm^{-1}), R (10^{-44} $esu^2 \cdot cm^2$), ξ (deg)

	freq	R	ξ
free BBA:	1157.71	−2.66	91.84
BBA−NH_3:	1156.99	6.55	69.65

(b) Im[$\vec{M}_{01}(i)$] (10^{-25} esu·cm)

	x	y	z
free BBA:	23.32	–124.62	41.98
BBA in MC:	−1.03	−65.47	34.91
NH_3 in MC:	0.47	−0.13	−0.73

(c) $\vec{E}_{01}(i)$ (10^{-21} esu·cm)

	x	y	z
free BBA:	−9.73	−19.24	−58.07
BBA in MC:	−12.98	−17.22	−13.66
NH_3 in MC:	−0.06	0.19	−0.07

(d) Contributions R^{ij} (10^{-44} $esu^2 \cdot cm^2$) of R

		R^{ij}	ξ (deg)
BBA in MC:	R^{AA}	6.64	69.48
coupling:	R^{AB}	0.06	73.95
coupling:	R^{BA}	−0.15	159.67
NH_3 in MC:	R^{BB}	0.00	92.18

[a] Ω is the normal mode's overlap; (a) frequencies (freq), rotational strength (R), and the angle ξ; (b and c) Cartesian components of the magnetic, $\vec{M}_{01}(i)$, and electric, $\vec{E}_{01}(i)$, dipole transition moments of free BBA, of BBA in BBA−NH_3, and of NH_3 in BBA−NH_3, respectively; (d) the contributions R^{AA}, R^{AB}, R^{BA}, R^{BB} to R of BBA−NH_3, and their associated angle ξ.

TABLE 4: Data Relevant for the Analysis of Pair 25 (Case B, Ω = 0.90) in Table 1[a]

(a) Frequency (cm^{-1}), R (10^{-44} $esu^2 \cdot cm^2$), ξ (deg)

	freq	R	ξ
free BBA:	1716.12	33.17	88.18
BBA−NH_3:	1676.06	−7.37	90.55

(b) Im[$\vec{M}_{01}(i)$] (10^{-25} esu·cm)

	x	y	z
free BBA:	328.42	119.35	421.91
BBA in MC:	367.66	178.98	324.60
NH_3 in MC:	−36.37	−10.62	−30.55

(c) $\vec{E}_{01}(i)$ (10^{-21} esu·cm)

	x	y	z
free BBA:	−24.93	−173.11	76.24
BBA in MC:	−20.16	−143.50	96.24
NH_3 in MC:	0.16	13.05	−1.51

(d) Contributions R^{ij} (10^{-44} $esu^2 \cdot cm^2$) of R

		R^{ij}	ξ (deg)
BBA in MC:	R^{AA}	−18.57	91.17
coupling:	R^{AB}	−6.83	94.63
coupling:	R^{BA}	19.01	73.90
NH_3 in MC:	R^{BB}	−0.98	98.82

[a] Ω is the normal mode's overlap; (a) frequencies (freq), rotational strength (R), and the angle ξ; (b and c) Cartesian components of the magnetic, $\vec{M}_{01}(i)$, and electric, $\vec{E}_{01}(i)$, dipole transition moments of free BBA, of BBA in BBA−NH_3, and of NH_3 in BBA−NH_3, respectively; (d) the contributions R^{AA}, R^{AB}, R^{BA}, R^{BB} to R of BBA−NH_3, and their associated angle ξ.

nuclear displacement vectors have been affected very little by the complexation. The frequency is also little changed. The rotational strength switches from small and negative in free BBA ($R = -2.66$ with $\xi = 91.84°$ only slightly larger than 90°) to small and positive ($R = 6.55$ with $\xi = 69.65°$ now clearly smaller than 90°). We have verified the magnitude of the atomic electric and magnetic dipole transition moments, and this change is brought about by the different contributions of the H_1 movement in the two cases. As can be seen in Table 3, the electric and magnetic transition moments in BBA−NH_3 and in BBA are rather different. Looking at the contributions of the rotational strength it can be seen that R^{AA} is the only important term. Because there are no contributions from the terms R^{AB}, R^{BA}, and R^{BB}, it is clear that the perturbation of the normal modes (that changed the transition dipole moments) is responsible for the change of the rotational strength. We have seen that the ξ angle is 91.84° in BBA, whereas in BBA−NH_3 it changes to 69.65°, leading to rotational strengths with different signs. This particular example shows that even a minor perturbation of a single atom (H_1) can change the magnitudes and in particular the (relative) orientation of the transition dipole moments, and therefore also the sign of the rotational strength.

As an example of the second case, where the coupling terms come into play, we consider the pair of modes with number 25, a typical C−O stretch of the carbonyl bond of the benzoyl group (C_1═O_2). The data relevant for the analysis of pair number 25 are given in Table 4. When going from the free molecule to the molecular complex, the frequency of the mode is red-shifted by approximately 40 cm^{-1} and the rotational strength turns from positive (33.17) to negative (−7.37). In both molecules (BBA and BBA−NH_3), the hydrogen atom H_1 is moving along with the carbonyl atoms, while the rest of the atoms of BBA are frozen. In the molecular complex, the motion of H_1 induces small movements of the NH_3 group. The displacement vectors therefore exhibit clear changes, though not very large: the overlap is still 0.90. Because the atoms in the intermolecular bonding area are moving in this normal mode, the changes in the APTs and AATs of these atoms upon complexation also play a role. Thus, both the atomic tensors and the nuclear displacements are responsible for the differences observed in the transition dipole moments. As can be seen, the transition dipole moments in BBA−NH_3 and in BBA differ, although still exhibiting similarities. Considering the various intrafragment and interfragment contributions, we note that the R^{AA} term in the complex indeed differs considerably from that in the free BBA and has a reversed sign (−18.57 vs 33.17). Analysis of the sign of this part of the rotational strength shows that in free BBA the angle ξ is 88.18° whereas in the molecular complex ξ is 91.17°. Changing the angle ξ by less than 3° is enough to change the sign of the rotational strength if the change is across the 90° value. We also note that the rather large transition dipole moments of BBA of this mode compensate the small value of cos ξ (ξ is close to 90°), and as a result the contribution R^{AA} of BBA to the rotational strength of the complex is rather large. The interfragment terms R^{AB} and R^{BA} have magnitudes comparable to the R^{AA} term. In particular, $R^{BA} = 19.01$ is significant. This can be understood from the fact that the angle (73.9°) deviates considerably from 90°, and as a result the inner product between the large BBA magnetic transition dipole moment and the small NH_3 electric transition dipole has a relatively large magnitude. The R^{BA} contribution of 19.01 would actually cancel the negative R^{AA} (−18.57) contribution. It is only through the

TABLE 5: Data Relevant for the Analysis of Pair 4 (Case C, Ω = 0.91) in Table 1[a]

(a) Frequency (cm^{-1}), R (10^{-44} $esu^2 \cdot cm^2$), ξ (deg)

	freq	R	ξ
free BBA:	920.55	−19.91	93.52
BBA−NH_3:	920.63	−44.03	95.62

(b) Im[$\vec{M}_{01}(i)$] (10^{-25} esu·cm)

	x	y	z
free BBA:	−280.51	130.22	−87.16
BBA in MC:	−337.94	147.12	−104.19
NH_3 in MC:	−1.32	1.01	1.81

(c) $\vec{E}_{01}(i)$ (10^{-21} esu·cm)

	x	y	z
free BBA:	54.52	69.15	−49.33
BBA in MC:	64.68	78.06	−60.53
NH_3 in MC:	0.00	−1.04	0.65

(d) Contributions R^{ij} (10^{-44} $esu^2 \cdot cm^2$) of R

		R^{ij}	ξ (deg)
BBA in MC:	R^{AA}	−40.67	95.16
coupling:	R^{AB}	−1.16	113.57
coupling:	R^{BA}	−2.21	118.15
NH_3 in MC:	R^{BB}	0.00	87.71

[a] Ω is the normal mode's overlap; (a) frequencies (freq), rotational strength (R), and the Angle ξ; (b and c) Cartesian components of the magnetic, $M_{01}(i)$, and electric, $\vec{E}_{01}(i)$, dipole transition moments of free BBA, of BBA in BBA−NH_3, and of NH_3 in BBA−NH_3, respectively; (d) the contributions R^{AA}, R^{AB}, R^{BA}, R^{BB} to R of BBA−NH_3, and their associated angle ξ.

TABLE 6: Data Relevant for the Analysis of Pair 2 (Case C, Ω = 0.97) in Table 1[a]

(a) Frequency (cm^{-1}), R (10^{-44} $esu^2 \cdot cm^2$), ξ (deg)

	freq	R	ξ
free BBA:	745.41	−44.26	98.06
BBA−NH_3:	752.99	−63.14	101.26

(b) Im[$\vec{M}_{01}(i)$] (10^{-25} esu·cm)

	x	y	z
free BBA:	73.46	−243.66	178.29
BBA in MC:	54.54	−245.47	195.40
NH_3 in MC:	13.21	−7.61	0.69

(c) $\vec{E}_{01}(i)$ (10^{-21} esu·cm)

	x	y	z
free BBA:	−94.36	−28.36	−24.70
BBA in MC:	−93.44	−18.11	−18.64
NH_3 in MC:	−0.02	−1.66	−6.79

(d) Contributions R^{ij} (10^{-44} $esu^2 \cdot cm^2$) of R

		R^{ij}	ξ (deg)
BBA in MC:	R^{AA}	−42.93	97.99
coupling:	R^{AB}	−11.09	138.55
coupling:	R^{BA}	−9.20	114.43
NH_3 in MC:	R^{BB}	0.08	85.87

[a] Ω is the normal mode's overlap; (a) frequencies (freq), rotational strength (R), and the Angle ξ; (b and c) cartesian components of the magnetic, $\vec{M}_{01}(i)$, and electric, $\vec{E}_{01}(i)$, dipole transition moments of free BBA, of BBA in BBA−NH_3, and of NH_3 in BBA−NH_3, respectively; (d) the contributions R^{AA}, R^{AB}, R^{BA}, R^{BB} to R of BBA−NH_3, and their associated angle ξ.

negative contribution of the R^{AB} term (−6.83) that the final rotational strength is negative. There is a minor contribution from the term R^{BB}, which involves only small transition moments.

Case **C** describes the pairs of normal modes that have VCD intensities of the same sign but of very different magnitudes. Our analysis showed that many of the modes in this case exhibit very similar perturbation patterns as the modes in case **B**. Again, many BBA modes in this case have values of the angle ξ that are close to 90°. However, unlike in case **B**, the perturbations induced by complexation in this case change ξ in the direction that preserves the sign of the rotational strength (if $\xi > 90°$ then it increases, if $\xi < 90°$ then it decreases). The same mechanisms described in case **B** are also responsible for changing the VCD intensities of the modes of this case; that is, we distinguish cases where coupling terms are not important and cases where they are.

As an example of the first case, we consider pair number 4. The modes are characterized by movements of the hydrogen atoms of the two benzene rings of BBA out of the planes of the benzenes they belong to. The hydrogen H_1 and the atoms of the NH_3 are frozen in both modes. Table 5 gives all of the information relevant for the analysis of this pair. The overlap of the normal modes is 0.91, which suggests that the BBA mode is still fully recognizable after the complexation. However, the change in the normal mode is enough to change the magnitude of Cartesian components of the electric and magnetic transition dipole moments of BBA in the molecular complex by 10 to 20% with respect to the free BBA. At the same time, the angle ξ has also changed from 93.52° to 95.16°. Although the changes are relatively small, the effects induced by complexation add up, resulting in an increased magnitude of the contribution R^{AA} by a factor of 2 with respect to the rotational strength of the free BBA, from −19.91 to −40.67. Because the NH_3 atoms move very weakly in this mode, they do not contribute much to the transition dipole moments, and the R^{BB} contribution (B stands for NH_3) as well as the contributions of the coupling terms R^{AB} and R^{BA} to the rotational strength are negligible.

As an example where coupling terms are important, we consider the normal modes pair number 2. The modes of pair 2 are characterized by movements of the hydrogen atoms of the benzoic acid out of the plane of the benzene ring they belong to. In free BBA, the hydrogen atom H_1 is moving with small amplitude. In BBA−NH_3, H_1 and the atoms of NH_3 are moving only slightly. All of the data relevant for the analysis of this pair are given in Table 6. The overlap of the normal modes is 0.97, indicating that the BBA mode was affected very little by complexation. The transition dipole moments also show relatively small differences, although the transition dipole moments (in particular the magnetic one) of the NH_3 fragment are now small but nonzero. The term R^{AA} and the rotational strength of the free BBA have approximately the same magnitude (−42.93 vs −44.26). This is also the case for the ξ angles associated with R^{AA} and with the rotational strength of the free BBA (97.99° vs 98.06°). Thus, it is clear that this particular normal mode of BBA was affected very little by the complexation with NH_3. However, because of couplings between the transition dipole moments of the two fragments, the rotational strength is not determined only by the term R^{AA}. The contributions R^{AB} and R^{BA} have the same order of magnitude as R^{AA} and the same sign. Note that although the angles between electric and magnetic transition dipole moments within either the BBA or

TABLE 7: Data Relevant for the Analysis of Pair 7 (Case D, Ω = 0.99) in Table 1[a]

(a) Frequency (cm^{-1}), R (10^{-44} $esu^2 \cdot cm^2$), ξ (deg)

	freq	R	ξ
free NH_3:	1033.1	0.00	90.00
BBA−NH_3:	1094.5	−36.79	94.05

(b) $\vec{M}_{01}(i)$] (10^{-25} esu·cm)

	x	y	z
free NH_3:	54.37	−20.72	244.12
NH_3 in MC:	106.21	−65.12	288.88
BBA in MC:	1.09	44.88	−14.01

(c) $\vec{E}_{01}(i)$ (10^{-21} esu·cm)

	x	y	z
free NH_2:	−13.18	−158.75	−10.54
NH_3 in MC:	−6.76	−183.07	−51.29
BBA in MC:	−0.81	8.80	28.03

(d) Contributions R^{ij} (10^{-44} $esu^2 \cdot cm^2$) of R

		R^{ij}	ξ (deg)
BBA in MC:	R^{AA}	0.01	89.94
coupling:	R^{AB}	74.40	36.44
coupling:	R^{BA}	−75.05	147.02
NH_3 in MC:	R^{BB}	−36.15	93.46

[a] Ω is the normal mode's overlap; (a) frequencies (freq), rotational strength (R), and the Angle ξ; (b and c) Cartesian components of the magnetic, $\vec{M}_{01}(i)$, and electric, $\vec{E}_{01}(i)$, dipole transition moments of free NH_3, of BBA in BBA−NH_3, and of NH_3 in BBA−NH_3, respectively; (d) the contributions R^{AA}, R^{AB}, R^{BA}, R^{BB} to R of BBA−NH_3, and their associated angle ξ.

the NH_3 fragments are close to 90°, the coupling terms are characterized by angles that are not close to 90°, so the cosine factor in the inner product may have much less effect. This can make inner products of small (for NH_3 fragment transition moments) times large (for BBA fragment transition moments) type of contributions still competitive with large times large (in R^{AA}) contributions. As a result, the coupling terms contribute significantly and the rotational strength is with approximatively 50% larger in the molecular complex than in the free molecule (−63.14 vs −44.26). This example highlights the sensitivity of the VCD intensities. Even weak coupling of an NH_3 mode to a predominantly BBA mode can have a large effect on the intensity.

Case **D** represents the modes of the achiral NH_3 that after the complexation with the chiral BBA have nonzero VCD intensities. This is a classical case of chirality transfer from the chiral BBA to the achiral NH_3.

As an example, the symmetric bend of NH_3 is considered (pair 7 in Table 1). In the free NH_3, this mode has a frequency of 1033 cm^{-1} and zero rotational strength, whereas in BBA−NH_3 the frequency of the mode is blue-shifted by 61 cm^{-1} and has a rotational strength of −36.79. In the molecular complex, with the exception of the atoms H_1 and O_1, which are moving very slightly, all of the other atoms of BBA are frozen. The data required for the analysis of this case are given in Table 7.

The correlation diagrams for all components of the APT and the AAT tensors of the NH_3 atoms in the free NH_3 and in the molecular complex are given in Figures 7 and 8, respectively. As can be seen in Figures 7 and 8, there are a number of points that deviate from the 45° line, indicating that some of the tensor components of both the APTs and the AATs have been perturbed during the process of complex formation. The normal mode's overlap is 0.99. Thus, although the frequency of the mode has shifted, the direction and magnitude of the displacement vectors were hardly affected by complexation.

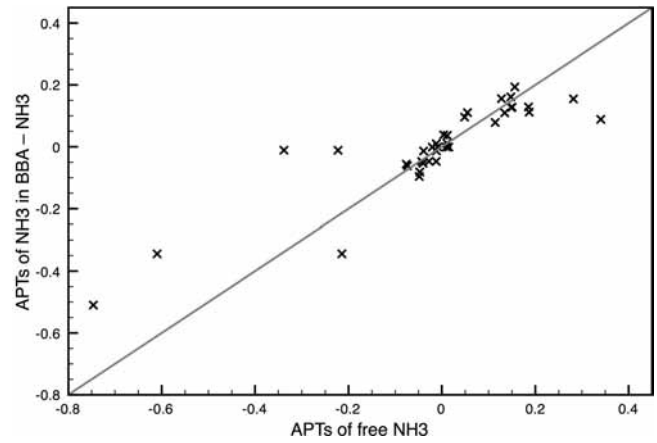

Figure 7. Correlation diagram for the tensor components of the APTs of the NH_3 atoms.

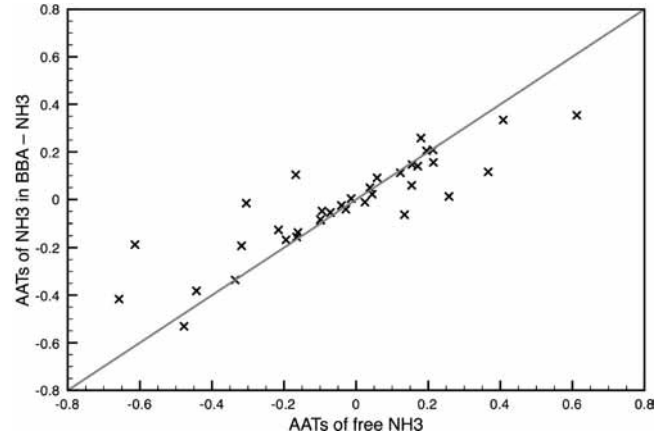

Figure 8. Correlation diagram for the tensor components of the AATs of the NH_3 atoms.

We continue with the investigation of the transition dipole moments. In achiral molecules, the electric and magnetic transition dipole moments associated with a vibrational transition of a normal mode are in general different from zero and perpendicular (by symmetry). As a result, their scalar product, which determines the rotational strength of that normal mode, is zero. As can be seen in Table 7, the transition dipole moments of the free NH_3 have nonzero magnitude and are indeed perpendicular. Looking at the transition dipole moments of the BBA−NH_3 complex, we see that their magnitudes have changed compared to the free NH_3 and that they are no longer perpendicular (ξ = 93.46°). This is a consequence of the perturbations of the atomic tensors: the normal mode has remained almost unchanged, but because the moving atoms are involved in the hydrogen bond, the electronic perturbation has affected the atomic tensors. As a result, the term R^{BB}, the contribution to rotational strength of BBA−NH_3 due to NH_3, is no longer zero (R^{BB} = −36.15). Looking at the other contributions to the rotational strength of BBA−NH_3 (Table 7), one can see that the term R^{AA} is negligible while the terms R^{AB} and R^{BA} have large magnitudes, indicating a strong coupling between the two monomers. Even though in this particular mode

TABLE 8: Frequencies and Rotational Strengths of the Bending Mode of Water in Free Water, Water−Methyl Lactate Complex, and Water−D-Lactic Acid Complex[a]

Methyl Lactate−Water
Frequency (cm^{-1}), R (10^{-44} $esu^2 \cdot cm^2$), ξ (deg)

	freq	R	ξ
free water:	1602.85	0.00	90.00
methyl lactate−water:	1620.81	64.06	79.04

Contributions to R (10^{-44} $cm^2 \cdot esu^2$)

		R^{ij}	ξ (deg)
methyl lactate in MC:	R^{AA}	3.22	95.04
coupling:	R^{AB}	−23.66	79.29
coupling:	R^{BA}	50.75	140.14
water in MC:	R^{BB}	33.73	98.46

D-Lactic Acid−Water
Frequency (cm^{-1}), R (10^{-44} $esu^2 \cdot cm^2$), ξ (deg)

	freq	R	ξ
free water:	1602.85	0.00	90.00
D-lactic acid−water:	1605.65	−152.48	106.21

Contributions R^{ij} (10^{-44} $esu^2 \cdot cm^2$) to R

		R^{ij}	ξ (deg)
D-lactic acid in MC:	R^{AA}	−0.94	91.74
coupling:	R^{AB}	−122.44	135.98
coupling:	R^{BA}	21.55	69.95
water in MC:	R^{BB}	−50.65	98.43

[a] The contributions R^{AA}, R^{AB}, R^{BA}, R^{BB} to the R of the molecular complex (MC) are also given. The BP86 functional and TZP basis set were used for the geometry optimizations and the VCD calculation. In the two molecular complexes, "B" labels the water while "A" labels either the methyl lactate or the D-lactic acid.

TABLE 9: Orbital Energies and Contributions (in Percent) of the MO σ^* (O_1 H_1) to the MO 58 of BBA−NH_3 for Various O_1−H_1 Bond Lengths (ΔR)[a]

MO	ΔR (Å)	E (eV)	%
σ^* (O_2 H_1)	+0.05	−0.82	5.6
σ^* (O_2 H_1)	0.00	−0.50	3.7
σ^* (O_2 H_1)	−0.05	−0.28	1.9
lone pair of NH_3		−6.15	
MO 58 of BBA−NH_3	0.00	−7.30	

[a] For comparison, the orbital energies of the nitrogen lone pair in the NH_3 and the corresponding MO 58 of BBA−NH_3 are also listed.

the terms R^{AB} and R^{BA} cancel each other, their large amplitude suggests that they can play an important role in chirality transfer phenomena.

In order to substantiate this remark, we consider the case of the water bending mode in the water−methyl lactate (experimentally measured in ref 14) and in the water−D-lactic acid (theoretically predicted in ref 12) complexes. Details regarding the structures of the two complexes and the parameters used in the calculations are given in the Supporting Information. Table 8 gives the contribution to rotational strengths of the binding mode of water in the two molecular complexes mentioned above. As can be seen, in both situations the interfragment terms R^{AB} and R^{BA} do not cancel each other anymore. Moreover, they have amplitudes that are comparable to or bigger than the term R^{BB} and contribute strongly to the large VCD intensities that were calculated and observed for the bending mode of water.

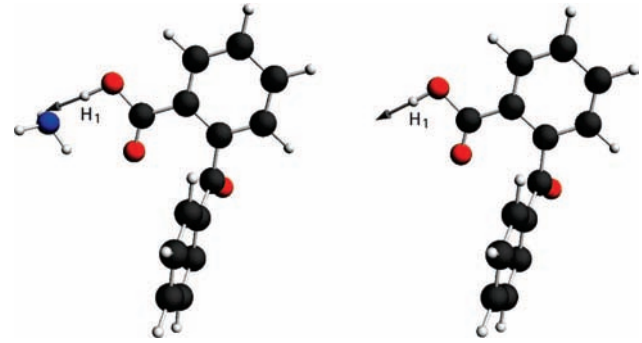

Figure 9. Nuclear displacement vectors for the normal modes of pair number 26 in Table 1.

TABLE 10: Data Relevant for the Analysis of Pair 26 in Table 1[a]

(a) Frequency (cm^{-1}), R (10^{-44} $esu^2 \cdot cm^2$), ξ (deg), γ

	freq	R	ξ	γ
free BBA:	3608.4	−7.99	91.75	
BBA−NH_3:	2588.9	−402.42	93.15	50
H_1:	2588.9	−400.81	93.4	50

(b) Electronic and Nuclear Conributions of $\mathrm{Im}[(M_{01}^{H_1})_y]$

	$(M_{01}^{H_1})_{nuc}$	$(M_{01}^{H_1})_{el}$	$(M_{01}^{H_1})_y$	γ
free BBA:	641.9	−400.2	241.7	
BBA−NH_3:	592.0	437.4	1029.5	4

(c) Electronic and Nuclear Conributions of $(E_{01}^{H_1})_y$

	$(E_{01}^{H_1})_{nuc}$	$(E_{01}^{H_1})_{el}$	$(E_{01}^{H_1})_y$	γ
BBA−NH_3:	217.9	80.8	298.7	7.5
free BBA:	197.4	−157.8	39.6	

[a] (a) Frequency and rotational strengths for modes of pair 26 in Table 1 calculated in free BBA, in BBA−NH_3, and using only the dipole transition moments of the atom H_1; (b and c) the projection on the y axis of the total electric, $(E_{01}^{H_1})_y$, and magnetic, $(M_{01}^{H_1})_y$ dipole transition moments, respectively, of the atoms H_1, and their electronic and nuclear contributions in the free BBA and in BBA−NH_3. γ is the ratio between the quantities R, $(E_{01}^{H_1})_y$ and $(M_{01}^{H_1})_y$, respectively, in the molecular complex and in the free molecule. Because $\tilde{M}_{01}(i)$ and its contributions are purely complex, their imaginary parts are given.

Case **E** describes the modes of pair number 26. These modes are O−H stretchings that exhibit a large frequency shift and a huge increase of the IR and VCD intensities when going from the free molecule to the molecular complex. As is known from IR spectroscopy,[30–32] such effects are encountered when the hydrogens participating in the stretching mode are involved in intra- or intermolecular bonds (the effects are more spectacular for the latter). The modes of pair 26 are depicted in Figure 9. As can be seen, the hydrogen atom H_1 (see Figure 1) that is involved in the intermolecular bond is indeed moving in these modes. In fact, it is the only atom moving with significant amplitude. In the following, the origin of the mechanism responsible for the enhancement of the VCD intensity is investigated. Next, its relation with the mechanism responsible for the enhancement of the IR intensities will be discussed.

In Table 10 the frequencies and the rotational strengths of the modes of pair 26 are given. In the molecular complex, the frequency of the mode is red-shifted by approximately 1000 cm^{-1} with respect to the value in free BBA, whereas the VCD intensity increases by a factor of approximatively 50, from −7.99 to −402.42. Because the hydrogen H_1 is the only atom

moving with significant amplitude (see Figure 9), the contributions from the rest of the atoms of BBA−NH_3 to the total electric and magnetic transition dipole moments are negligible. The rotational strength calculated using just the transition dipole moments of the hydrogen H_1 is also given in Table 10. The obtained value, 400.81, represents 99.59% of the total rotational strength (which is 402.42). Thus, in what follows only the electric and magnetic transition dipole moments of this hydrogen atom will be considered.

The rotational strength of the molecular complex can be decomposed into x, y, and z contributions

$$R = R_x + R_y + R_z = \mathrm{Im}(E_x M_x + E_y M_y + E_z M_z) \quad (16)$$

where E_k and M_k (with $k = x, y, z$) are the Cartesian components of the electric (E_{01}) and magnetic (M_{10}) transition dipole moments, respectively.

In the molecular complex, all of these contributions increase significantly compared to their values in the free BBA; the factors are 10, 30, and 33, respectively. Because R_x, R_y, and R_z do not all have the same sign, an overall increase by a factor of 50 is obtained. As an example, we analyze the R_y contribution in detail. In Table 10, the nuclear and electronic contributions of the y components of the electric and magnetic transition dipole moments of the modes in pair 26 are given. As can be seen, the nuclear contributions of the electric and magnetic transition dipole moments have about the same magnitude and the same sign in the free molecule and in the molecular complex. The electronic contributions, however, have different signs. Thus, in BBA the electronic and the nuclear components of the two transition dipole moments have different signs and therefore counteract each other, whereas in BBA−NH_3 they reinforce each other because they have the same sign. As a result, the y components of the two transition dipole moments increase in the molecular complex when compared to the free molecule by a factor of 4 in the case of the magnetic transition dipole moment and by a factor of 7.5 in the case of electric transition dipole moment. This implies an increase of the contribution $R_y = \mathrm{Im}(E_y M_y)$ of the rotational strength of the molecular complex by a factor of 30. This leads us to the conclusion that the observed sign change of the electronic contributions of the two transition dipole moments is responsible for the increase of the VCD intensities. Because the IR intensities are determined by the electric transition dipole moments (E_{01}) via the dipole strengths, $D(i) = |E_{01}(i)|^2$, the same mechanism is responsible for their enhancement.

Furthermore, the origin of the large changes in the electronic parts of the transition dipole moments is investigated. From eqs 4 to 9, the electronic contributions to the electric and magnetic transition dipole moments of a single atom (λ) are given by

$$(E_{01}^{\lambda})_{\beta}(i) = \left(\frac{\hbar}{\omega_i}\right)^{1/2} \sum_{\alpha} E_{\alpha\beta}^{\lambda} S_{\alpha}^{\lambda}(i) \quad (17)$$

$$(M_{10}^{\lambda})_{\beta}(i) = -(2\hbar^3\omega_i)^{1/2} \sum_{\alpha} I_{\alpha\beta}^{\lambda} S_{\alpha}^{\lambda}(i) \quad (18)$$

where $E_{\alpha\beta}^{\lambda}$ and $I_{\alpha\beta}^{\lambda}$ are the electronic contribution of APTs and AATs, respectively. The correlation diagrams for the electronic contributions of the nine components of the APT and the AAT of the hydrogen H_1 in BBA and in BBA−NH_3 are given in Figures 10 and 11, respectively. The correlation diagrams of both atomic tensors ($E_{\alpha\beta}^{\lambda}$, $I_{\alpha,\beta}^{\lambda}$) show large deviations from the 45° line. Alternatively, the overlap of the displacement vectors of H_1 in BBA and in BBA−NH_3 is 0.99. Thus, it is clear that the perturbations induced in the atomic tensors are responsible

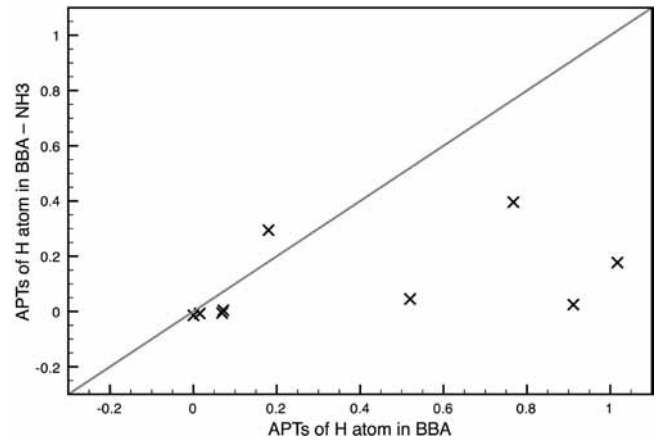

Figure 10. Correlation diagram for the nine tensor components of the electronic APT of the hydrogen H_1 in Figure 1.

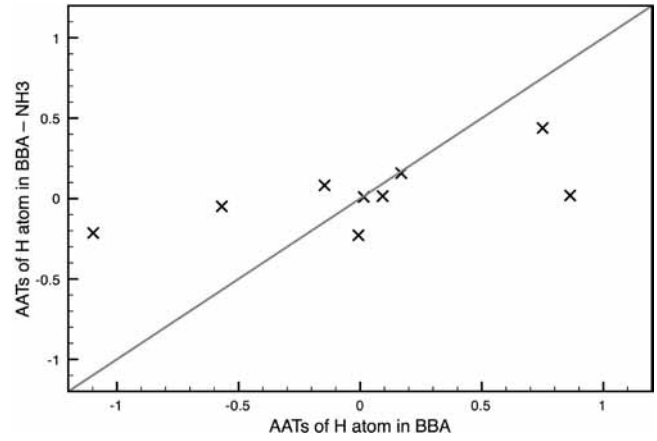

Figure 11. Correlation diagram for the nine tensor components of the electronic AAT of the hydrogen H_1 in Figure 1.

for the observed sign change of the electronic contributions of the two transition dipole moments and therefore for the enhancements of the IR and VCD intensities.

The electronic contributions of both the APTs and AATs can be written in terms of contributions from the occupied molecular orbitals (MO); see eqs 25 and 28 in ref 25 for more details. The contributions from the occupied MOs of all of the tensor components of the APTs and the AATs in BBA and in BBA−NH_3 have been investigated carefully. We found that the contribution due to the MO number 58 of BBA−NH_3 is alone responsible for the differences between the atomic tensors of the hydrogen atom H_1. Among the MOs of the two monomers that are combined into MO 58 of BBA−NH_3, the most important ones for understanding the enhancement of the IR and VCD intensities are the lone pair of the NH_3 and an unoccupied σ^* MO of BBA. The σ^* MO is localized on the O_1−H_1 bond. The lone pair contributes to the MO 58 with 63%, whereas the σ^* does so with 3.7%. This is a typical case of donor−acceptor interaction between the filled nitrogen lone pair as donor and the σ^* (O_1 H_1) as acceptor, as depicted in the MO interaction diagram of Figure 12. The amount of charge transfer in this interaction sensitively depends on the relative energies of these orbitals, notably on the orbital energy of the σ^* (O_1 H_1), which in turn depends strongly on the length of the O_1−H_1 bond. To monitor the charge flow, the hydrogen atom H_1 was displaced from its equilibrium position by $\Delta R = 0.05$ Å along its nuclear displacement vector in both directions. For each displacement, a single point calculation in the unrelaxed geometry was done. The effects of the displacements on the σ^*

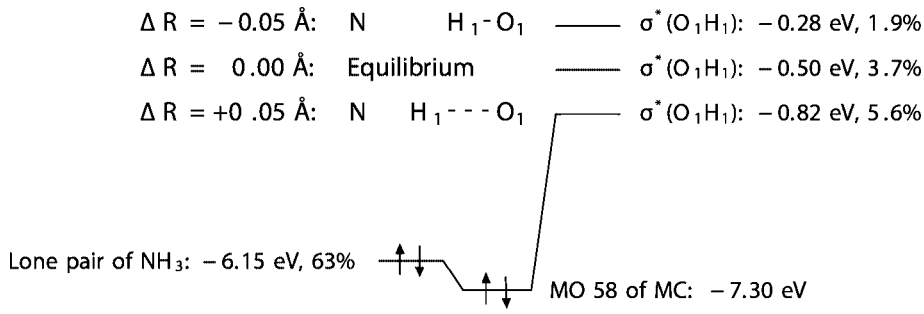

Figure 12. Mixing of the σ^* (O_1 H_1) orbital with the NH_3 lone pair for various O_1-H_1 bond lengths (ΔR).

(O_1 H_1) MO are summarized in Table 9 and Figure 12. When the hydrogen is moving away from the oxygen ($\Delta R = +0.05$ Å) the energy of σ^* (O_1 H_1) is going down, getting closer energetically to the lone pair of NH_3 and as a result σ^* (O_1 H_1) mixes more into MO 58. When the hydrogen is moving toward oxygen ($\Delta R = -0.05$ Å), the energy of the σ^* (O_1 H_1) is going up and thus σ^* (O_1 H_1) mixes less into the MO 58. This means that there is increased charge flow into the σ^* (O_1 H_1) and increased bonding to the nitrogen when the O_1-H_1 bond is stretched. Thus, the O_1-H_1 bond is weakened, which explains the observed red-shift of the frequency. Using the contributions (in percent) of the σ^* MO to MO 58 from Table 9, it was calculated that the amount of charge that flows into the O_1-H_1 bond region upon varying the bond distance by $\Delta R = 0.1$ Å is $\Delta q = 0.037$ electrons. This may seem to be a small amount of charge. However, because the charge travels over a large distance, the change induced in the electric dipole moment will be very large. As a qualitative test, the variation of the electric dipole moment created due to a transfer of a charge $\Delta q = 0.037$ electrons over a distance $R_{NO} = 2.67$ Å, which represents the $N-O_1$ distance, was calculated by a finite difference approximation:

$$\frac{\partial \mu_E}{\partial R_H} = \frac{\Delta q R_{NO}}{\Delta R} = 0.99 \text{ au} \qquad (19)$$

The tensor components of the APT represent the derivatives of the electric dipole moment with respect to a nuclear displacement. Thus, the result of eq 19 is compared to the difference between the value of electronic contributions of the APT of the hydrogen H_1 in $BBA-NH_3$ (MC) and in free BBA (FM) (note that the vector determined by the position of the atoms O_1 and N is along the y axis):

$$\left[\frac{\partial (\mu_E^{H_1})_y}{\partial R_y^{H_1}}\right]_{MC} - \left[\frac{\partial (\mu_E^{H_1})_y}{\partial R_y^{H_1}}\right]_{FM} = E_{yy}^{H_1}(MC) - E_{yy}^{H_1}(FM) = 1.27 \text{ au} \qquad (20)$$

Analytical derivative techniques have been employed for the calculation of both Eyy^{H1} tensor components in eq 20. As can be seen from eqs 19 and 20, the accurate analytical calculation is well approximated by the estimation from the finite difference calculation. This clearly shows that the difference in the dipole moment derivatives for complex and free molecules can be explained by the simple model of $O-H_1$ distance-dependent transfer of charge from the lone pair of NH_3 into the O_1-H_1 bond region. The large dipole moments created by this charge transfer are responsible for the observed change of the sign of the electronic contributions of the electric and magnetic transition dipole moments and, thus, for the enhancement of the IR and VCD intensities. We note that the data in Table 10 can be given a very simple and intuitive physical interpretation. The fact that in the free BBA the nuclear and electronic contributions of the electric and magnetic transition dipole moments of the H_1 atom have different signs indicates that the displacement of the nucleus H_1, signifying a movement of the positive nuclear charge, is counteracted by the movement of the negative electronic charge that it drags along. However, the charge transfer from the lone pair of the NH_3 into the σ^* is an opposite movement of negative electronic charge, explaining the change of sign for the electronic contribution of the two transition dipole moments in the molecular complex, and in turn the intensity enhancement.

The enhancement of the VCD intensity in the calculations is very striking. It raises the question whether it could be observed experimentally. Of course, the hydrogen-bonded complexes do not have very rigid structures, so the solvent molecules will sample a range of orientations relative to the solute, each of them with a different frequency shift, and a different intensity. Furthermore, the angle ξ for the O−H stretching mode studied here ($O_1-H_1\cdots N$) is very close to 90° ($\xi = 93.15°$). This suggests that slightly different orientations of the two monomers with respect to each other can result in rotational strengths of different signs. Therefore, it will be interesting to search for experimental verification of the effect described here.

The mechanism for intensity enhancement we have identified for this intermolecular hydrogen bond may also work for other bonds of donor−acceptor type. We note that Sadlej et al.[12] observed in their DFT calculations a significant increase (10-fold) of the rotational strength of a C═O mode in $O-H\cdots O{=}C$ hydrogen-bonded systems. We have calculated and analyzed the VCD intensity of the respective mode, and indeed the same mechanism described here is responsible for the enhancement.

Finally we would like to note that, like in the case of chirality transfer (case **D**), the cross terms R^{BA} and R^{BA} are not directly responsible for the enhancement of the VCD intensity. However, because in general they are not zero, they can further affect the rotational strength of the molecular complex.

Case **F** describes the normal modes that are specific either to BBA or to $BBA-NH_3$. In Table 1, three examples of modes of this type are given (mode numbers 14, 16, and 19). It should be noted that these modes are not intermolecular modes (the six additional modes that appear in the molecular complex). They are the result of the perturbation induced by the complexation with NH_3, which causes some of the modes of the free BBA to mix. Thus, these modes are just linear combinations of modes of free BBA. Because the structures of BBA and $BBA-NH_3$ considered in this work are chiral, the electric and magnetic transition dipole moments of these modes are usually not perpendicular and therefore they usually have nonzero VCD intensities. As can be seen in Table 1, all three modes considered here have relatively large VCD intensities. This clearly shows

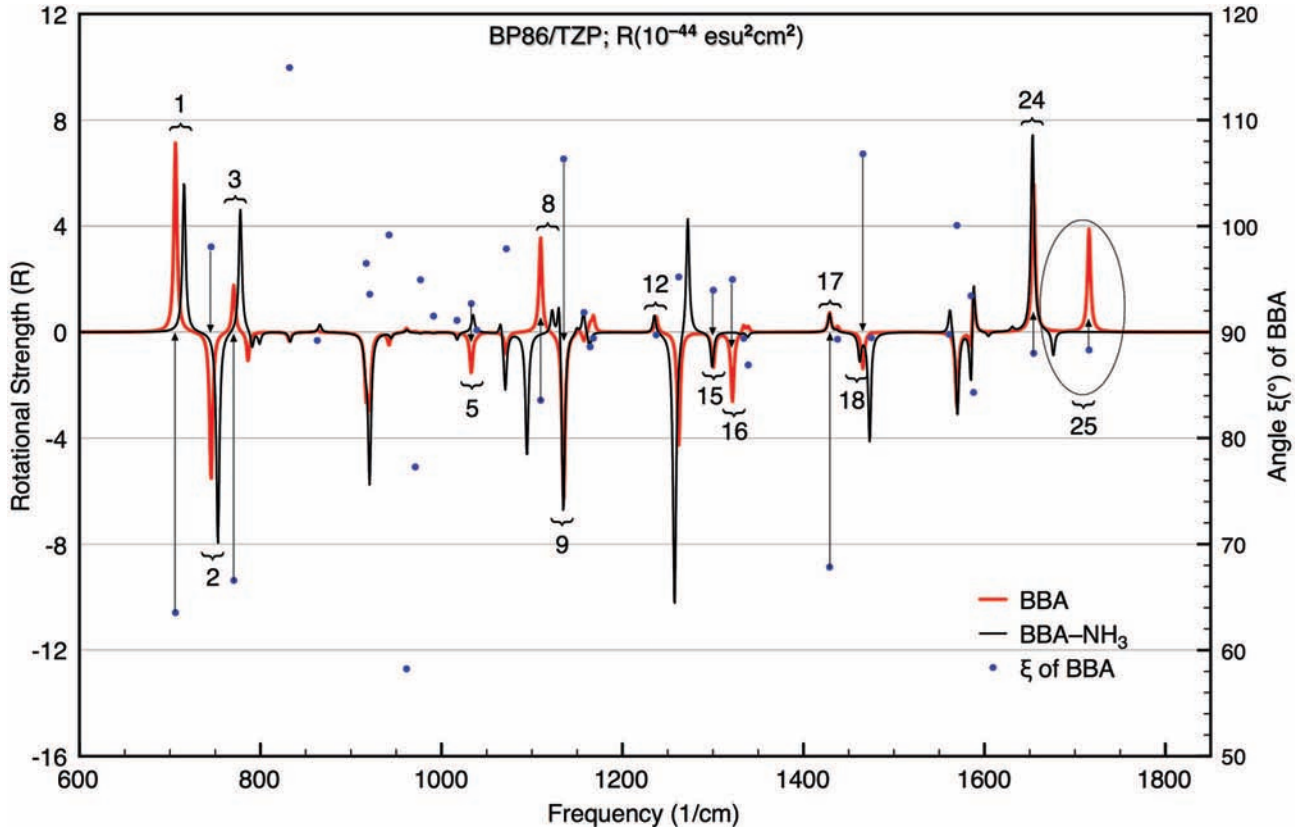

Figure 13. VCD spectra (BP86/TZP) of BBA and BBA−NH_3 and the angles ξ of the modes of BBA.

that this mixing of modes can change the shape of the VCD spectra significantly. Unfortunately, if such modes are present in the experimental spectrum, then it is very difficult to identify and resolve them without knowing exactly the type of perturbation/interaction that produced them.

Summary and Conclusions

An experimental VCD spectrum of a molecule in solution will include the perturbations due to complexation with solvent molecules, whereas such perturbations are absent in the VCD calculation on the isolated molecule. In this work, we have theoretically investigated the various effects of complexation in order to determine when significant deviations of the calculated signals from the experimental ones due to the solvent effects in the latter can be expected. The most important conclusion is that VCD signals can be classified as *robust*, that is, not (much) susceptible to change their sign due to solvation, when the angle between the electric and magnetic transition dipoles of the corresponding vibrational mode are significantly different from 90°. This can be displayed effortlessly as a standard result from the theoretical calculation and can be indicated for each mode in the simulated spectrum, for instance as a dot indicating the magnitude of the angle, see Figure 13. Using the baseline as the 90° line (see the vertical right axis for the angle), dots that center around the baseline in a band of ±10° point to modes that are not robust. A sign change of their rotational strength will occur if the angle ξ between the electric and magnetic dipole moments changes across 90°. When ξ is very close to 90°, the sign of the rotational strength will sensitively depend either on the computational parameters (basis sets, functional, geometry, etc.) or on the perturbations that may be present in the experiment (solvation, hydrogen bonding, etc.). We caution against overinterpreting discrepancies between (gas phase) theory and (solution) experiment for such nonrobust modes. It is the robust modes that should be singled out for determination of the absolute configuration. Such modes have to be determined by the angle ξ differing from 90° by more than 20° for example, they cannot be distinguished by just a large intensity (large rotational strength). For instance, modes 5, 8, 16, and 25 have reasonable intensity, but are not robust and do change upon complexation. This then should be of no concern when comparing experiment and theory. Of course, nonrobust modes do not *have* to change; some (e.g., 12, 15, 24) are unaltered. Robust modes, with angles outside the 70−110° window (more studies are needed to determine an appropriate interval), should be characteristic, and their sign should not change upon complexation. This holds true for modes like the intense 1, 3, and 9 and the weak 17 and 18.

The role of the angle ξ can be highlighted with the results of our analyses. We have distinguished the cases **A**−**F** to denote the various situations encountered. Case **A** represents the normal modes with VCD signals that are unaffected by complex formation. These modes are localized far from the intermolecular bond and do not involve the atoms in the intermolecular bond.

The analysis of cases **B** (change of sign) and **C** (significant change in magnitude) showed that there are two distinct mechanisms that can alter the VCD intensities when going from the free molecule to the molecular complex: (A) Perturbations of the normal modes of the chiral molecule and/or its APTs and AATs. In this case, the intrafragment contribution R^{AA} (*A* is BBA) to the rotational strength of the complex is the only significant contribution and has different magnitude compared to the isolated molecule. (B) Couplings between electric and magnetic transition dipole moments of the two monomers (in this case the interfragment contributions R^{AB} and R^{BA} (*B* is NH_3) have the same order of magnitude as R^{AA} and therefore play an

important role. These mechanisms may occur in both cases **B** and **C**; the only significant difference is the direction in which the angle ξ changes in response to the perturbation induced by complex formation, that is, crossing 90° (case **B**) or not crossing 90° (case **C**). The analysis of pair 25 (case **B**) showed that even variations of less than 3° of the angle ξ can cause the rotational strength to change sign. The analysis of pair number 10 (case **B**) showed that even small perturbations of the displacement vectors of a single atom can significantly change the magnitude of the dipole transition moments and therefore the angle ξ. The analysis of pairs 25 (case **B**) and 26 (case **E**) showed that rotational strengths can have large magnitudes even when ξ is close to 90°.

In case **D**, where modes of the achiral NH_3 show nonzero VCD intensities in the molecular complex ("transfer of chirality"), the perturbations induced by the complexation with BBA cause the electric and magnetic transition dipole moments of the modes of the NH_3 fragment to no longer be perpendicular, with a nonzero intrafragment VCD intensity ($R^{BB} \neq 0$) as a result.

Case **E** is the special effect that a giant enhancement of VCD intensity is calculated for the stretching mode of the O−H involved in the hydrogen bond. We have analyzed this in detail and have shown that it is due to the donor−acceptor interaction between the two monomers.

Lastly, we have also met case **F**, where peaks in the VCD spectrum of the solvated molecule cannot be reproduced or deduced from calculations performed on the isolated solute molecule alone. Such VCD peaks arise in the experimental spectrum due to mixing of modes of the solute caused by the complexation with a solvent molecule.

Our analysis of the mechanisms that change the VCD signals prove that treating the solvent as a structureless continuum is not a good approximation for VCD calculations if complex bonds between the solute and solvent molecules exist.

Finally, we note that the effects we have been describing arise from the molecular interaction between a chiral (BBA in a fixed conformation) and a nonchiral molecule (NH_3), but will not be different when both molecules are chiral. Exactly the same mechanisms will be operative, only the "transfer of chirality" of course will not occur, only perturbation of modes of the two chiral moieties.

Acknowledgment. J.N. thanks Prof. M. Reiher for generous support and acknowledges funding by a Liebig-Stipendium of the Fonds der Chemischen Industrie.

Supporting Information Available: Computational details and VCD analysis. This information is available free of charged via the Internet at http://pubs.acs.org.

References and Notes

(1) Freedman, T. B.; Cao, X.; Dukor, R. K.; Nafie, N. A. *Chirality* **2003**, *15*, 734–758.
(2) Cheesman, J. R.; Frisch, M. J.; Devlin, F. J.; Stephens, P. J. *Chem. Phys. Lett.* **1996**, *252*, 211–220.
(3) Jalkanen, K.; Suhai, S. *Chem. Phys.* **1996**, *208*, 81–116.
(4) Wang, F.; Polavarapu, P. L. J. *Phys. Chem. A* **2000**, *104*, 1822–1826.
(5) Burgi, T.; Vargas, A.; Baiker, A. *J. Chem. Soc., Perkin Trans.* **2002**, *2*, 1596–1601.
(6) Rode, J. E.; Dobrowolski, J. C. *J. Mol. Struct.: THEOCHEM* **2003**, *637*, 81–89.
(7) Cappelli, C.; Monti, S.; Rizzo, A. *Int. J. Quantum Chem.* **2005**, *104*, 744–757.
(8) He, J.; Polavarapu, P. L. *J. Chem. Theory Comput.* **2005**, *1*, 506–514.
(9) Kuppens, T.; Herrebout, W.; van der Veken, B.; Bultinck, P. *J. Phys. Chem. A* **2006**, *110*, 10191–10200.
(10) Freedman, T. B.; Cao, X.; Phillips, L. M.; Cheng, P. T. W.; Dalterio, R.; Shu, Y.; Zhang, H.; Shukla, R. B.; Tymiak, A.; Gozo, S. K.; Nafie, L. A.; Gougoutas, J. Z. *Chirality* **2006**, *18*, 746–753.
(11) Jürgensen, V. W.; Jalkanen, K. *Phys. Biol* **2006**, *8*, S63–S79.
(12) Sadlej, J.; Dobrowolsky, J. C.; Rode, J. E.; Jamroz, M. H. *Phys. Chem. Chem. Phys.* **2006**, *8*, 101–113.
(13) Zhang, P.; Polavarapu, P. L. *J. Phys. Chem. A* **2007**, *111*, 858–871.
(14) Losada, M.; Xu, Y. *Phys. Chem. Chem. Phys.* **2007**, *9*, 3127–3135.
(15) Sun, W.; Wu, J.; Zheng, B.; Zhu, Y.; Liu, C. *J. Mol. Struct.: THEOCHEM* **2007**, *809*, 161–169.
(16) Han, W.; Jalkanen, K.; Elstner, M.; Suhai, S. *J. Phys. Chem. B* **1998**, *102*, 2587–2602.
(17) Jalkanen, K.; Degtyarenko, I. M.; Nieminen, R. M.; Cao, X.; Nafie, L. A.; Zhu, F.; Barron, L. D. *Theor. Chem. Acc.* **2008**, *102*, 2587–2602.
(18) Takenaka, S.; Kondo, K.; Tokura, N. *J. Chem. Soc., Perkin Trans. 2* **1975**, 1520–1524.
(19) Neugebauer, J.; Baerends, E. J. *J. Phys. Chem. A* **2006**, *110*, 8786.
(20) Stephens, P. J. *J. Phys. Chem.* **1985**, *89*, 748–752.
(21) Stephens, P. J. *J. Phys. Chem.* **1987**, *91*, 1712–1715.
(22) te Velde, G.; Bickelhaupt, F. M.; Baerends, E. J.; Guerra, C. F.; van Gisbergen, S. J. A.; Snijders, J. G.; Ziegler, T. *J. Comput. Chem.* **2001**, *22*, 931–967.
(23) Guerra, C. F.; Snijders, J. G.; te Velde, G.; Baerends, E. J. *Theor. Chem. Acc.* **1998**, *99*, 391–403.
(24) *Amsterdam Density Functional Program*; Theoretical Chemistry, Vrije Universiteit: Amsterdam; URL: http://www.scm.com.
(25) Nicu, V. P.; Neugebauer, J.; Wolff, S. K.; Baerends, E. J. *Theor. Chem. Acc.* **2008**, *119*, 245–263.
(26) Swart, M.; Bickelhaupt, F. M. *J. Comput. Chem.* **2007**, DOI 10.1002/jcc.20834.
(27) Gerratt, J.; Mills, I. *J. Chem. Phys.* **1968**, *49*, 1719–1729.
(28) Pople, J. A.; Krishnan, R.; Schlegel, H. B.; Binkley, J. S. *I. J. Quantum Chem.: Quantum Chem. Symp.* **1979**, *13*, 225–241.
(29) Wolff, S. K. *Int. J. Quantum Chem.* **2005**, *104*, 645.
(30) Pimetel, G. C.; McClellan, A. L. *The Hydrogen Bond*; W. H. Freeman and Company: San Francisco, CA, 1960.
(31) Davies,M., Ed. *Infra-red Spectroscopy and Molecular Structure*; Elsevier Publishing Company: Amsterdam, 1963.
(32) Schuster,P.; Zundel, G.; Sandorfy, C., Eds. North-Holland: Amsterdam, 1976; Vols. *I*−*III*.
(33) Stephens, P.; Devlin, F. *Chirality* **2000**, *12*, 172–179.
(34) Freedmann, T. B.; Cao, X.; Dukor, R. K.; Nafie, L. A. *Chirality* **2003**, *15*, 743–758.

JP710201Q